J Therm Anal Calorim (2015) 119:1339–1352
DOI 10.1007/s10973-014-4230-4

Investigation of thermally induced processes in corundum refractory concretes with addition of fly ash

Anja Terzić · Nina Obradović · Ljubiša Andrić · Jovica Stojanović · Vladimir Pavlović

Received: 27 January 2014 / Accepted: 4 October 2014 / Published online: 19 October 2014

Abstract The effects that the fly ash addition has on the behavior of thermally resistant corundum concrete were discussed. Experimental program implied production of two refractory composites: "referent" concrete from 20 % of high-aluminate cement and 80 % of corundum aggregate, "recycled" concrete from 10 % of high-aluminate cement, 20 % of lignite coal ash, and 70 % of corundum aggregate. The fly ash was mechanically activated by a vibratory disk mill. In the concrete matrix, the ash had a role of cement partial replacement and microfiller. The mechanical and thermal properties of the concretes were studied at temperatures ranging from ambient to 1,400 °C as adopted maximum. Mechanisms of thermally induced processes were observed by differential thermal analysis at 10, 20, and 30 °C min^{-1} heating rates. Referent and recycled concretes showed differences in calculated activation energies. The variations in refractory concretes performances were discussed with support of scanning electron microscope imagining and X-ray diffraction results. The recycled ash concrete exhibited properties that met the requirements for the castables, which proves it suitable for use in severe conditions at high temperature and highlights the reusing principle and possibility of cleaner and economically sustainable production.

Keywords Mechanical activation · Powder processing · Composites · Dehydration · Sintering · Activation energy

Introduction

Refractory concretes are normally employed in the construction of metallurgical furnaces and structures that undergo cyclic thermal loading (e.g., linings in blast furnaces, steel making ladles, electricity producing reactors, etc.) [1]. Depending on the conditions of use, a number of factors influence cracking and breaking point of the refractory concretes: oxidation due to high temperature and air interaction, erosion due to the movement of molten fluids, microstructure differential expansion, and macroscopic thermo-mechanical stress induced by the thermal gradient [2]. The failure mechanism of a refractory concrete is significantly more complex than that of standard building concrete. The sintering present in refractory material is a process which makes difference in behavior of standard and refractory concretes. While mechanical characteristics (compressive strength, flexural strength, etc.) are the most important parameters in the characterization of a standard concrete, in the investigation of refractory concrete, special attention has to be paid on the behavior during and/or after exposure to high temperatures, since the temperature gives the final shape to the characteristics and the performance of a refractory concrete [3].

The refractory concretes are composed of refractory cement or an affine binder, and temperature-resistant aggregates. However, it is not uncommon that additives or

A. Terzić (✉)
Institute for Material Testing, Vojvode Mišića Boulevard 43, Belgrade, Serbia
e-mail: anja.terzic@institutims.rs

N. Obradović · V. Pavlović
Institute of Technical Sciences, Serbian Academy of Science and Art, Knez Mihailova St. 35, Belgrade, Serbia

L. Andrić · J. Stojanović
Institute for Technology of Nuclear and Other Raw Mineral Materials, Franchet d'Esperey St. 86, Belgrade, Serbia

partial replacements of standard raw materials are included in certain amounts in order to improve the flowability of the mixture, or a chemical, physical, or mechanical property of the hardened composite [4]. The fly ash, same as other coal combustion by-products, is commonly being applied in a large variety of engineering applications. There is a considerable amount of literature on the sintering of fly ash highlighting the positive influence of the thermal treatment on the mineralogical, chemical, physical, and mechanical properties and justifying the application of fly ash in the refractory concrete [5–10]. Namely, since the fly ash shows adequate behavior at elevated temperatures, it can be used as a partial replacement of cement or microfiller in the design of refractory concretes [11, 12].

Mechanical activation is a procedure which is often applied as a means of improvement of the fly ash performing characteristics in mix-design of a concrete. The mechanical activation of solid substance is achieved through fine and ultra-fine processing of the powdery material in the specially designed high-energy mills [13]. The activated state of an inorganic solid material occurs as a consequence of the specific surface area increase, and appearance and subsequent concentration of the atomic defects and dislocations [14]. Activation does not only affect the change of the particle size, it is also a complex chemico-physical process which induces the increase of potential energy, chemical activity, and surface reactivity of treated system. During mechanical activation, the reactive capabilities and structural parameters of the activated material are changing due to the excess of free energy making a potential center for forming of a new phase [15, 16]. Therefore, the activation, as a means of increasing of material reactivity, can be successfully utilized in optimization and rationalization of a variety of high-temperature basic production technologies including sintering. The purpose of mechanical activation as a precursor for sintering is to reduce the sintering temperature and to accelerate the process.

In this study, the effectiveness of mechanical activation of fly ash as a component in refractory concrete production was investigated through experimental program. Two types of corundum-based refractory concretes were prepared. Activated fly ash was added as cement replacement and microfiller in the mix-design in one of the concretes. High-temperature behavior and sintering processes of both concretes were investigated and compared. The performance of a concrete was determined in terms of compressive and flexural strength, porosity, refractoriness, and refractoriness under load. The goal was to obtain the refractory concrete based on secondary raw material which would have matching mechanical and thermal properties to those of standard refractory concrete.

Experimental

Materials and methods

The two types of the refractory concretes were prepared for the investigation: ordinary refractory concrete (C) and refractory concrete with addition of fly ash (CFA). The research was conducted with the purpose to study the influence of the ash addition on the thermally induced properties of refractory concrete. The concrete specimens were based on of the same type of refractory aggregate—corundum (fused alumina; MOTIM Fused Cast Refractories Ltd., Hungary) and the same refractory binder—high-aluminate cement Secar 71 (Lafarge, France) as it was used in our previous investigation [17]. A solid powdery chemical admixture Litopix–P56 (Zschimmer & Schwarz, Germany) was added to improve the workability of the concrete mixture. Fly ash was utilized in the mix-design of the CFA refractory concrete as partial replacement of the cement and at the same time as microfiller. The chemical compositions of the applied components as well as the compositions of the obtained refractory concretes are given in Table 1. The chemical analyses were performed by atomic emission spectroscopy technique on a PinAAcle 900 atomic absorption spectrometer (Perkin Elmer, USA). The loss of ignition (LoI) was determined by the mass difference between temperature 20 and 1,000 °C.

The applied fly ash is a by-product of the combustion of lignite coal from the "Kolubara" power plant in Serbia. The fly ash was collected directly from the filter system and transported to a closed silo where a sample of 500 kg of ash was randomly taken and re-sampled by the quarter method obtaining smaller samples which were preserved in hermetically sealed boxes until further investigation. The chemical analysis confirmed that the fly ash belongs to F class according to the ASTM C 618. The particle size gradings of the original ash sample varied in a wide range from 0.1 m^{-6} to 2.0 m^{-3} as it was also found in our previous investigation [12]. The fly ash particle size grading curve is given in Fig. 1 in "Results and discussion" section.

The fly ash was submitted to mechanical activation treatment before mixing with refractory cement in order to achieve smaller particle sizes, to improve specific surface area and over-all fineness-related characteristics. A number of laboratory mills can be utilized in the process of the powdery material activation: conventional ball mills, where mechanical energy is transferred on to batch by centrifugal, gravitational, and frictional forces; vibratory/planetary/centrifugal mills with peripheral comminuting path, where energy is transferred directly on to activating elements; and stream mills, where gas stream kinetic energy is transferred on to processed material [18–22]. In this investigation, a vibratory disk mill Siebtechnik-TS750 (Siebtechnik, Germany) is applied for the ash activation procedure. The feed size of the TS750 mill is 5–15 m^{-3};

Table 1 Chemical composition of components and concretes

Oxide/%	Cement	Fly ash	F class FA[a]	Corundum	Admixture[b]	C	CFA
SiO_2	0.15	55.15	>70 %	0.05	4.00	0.08	0.15
Al_2O_3	71.02	19.32		99.55	24.00	94.32	90.92
Fe_2O_3	0.18	5.98		0.05	–	0.09	0.13
TiO_2	0.01	0.55	–	0.01	–	0.02	0.04
CaO	27.35	7.95	<10 %	0.02	–	5.05	6.51
MgO	0.25	2.98	<5	–	19.00	0.05	0.93
P_2O_5	–	0.05	–	–	–	–	0.01
SO_3	–	0.75	<5 %	–	–	–	–
Na_2O	0.20	0.65	–	0.20	33.00	0.24	1.1
K_2O	0.01	1.65	–	–	–	–	–
MnO	–	0.03	–	–	–	–	–
CO_2	–	0.25	–	–	–	–	–
LoI	0.83	4.94	<6 %	0.12	20.00	0.15	0.21

[a] Classification according to ASTM C 618; [b] Provided by manufacturer

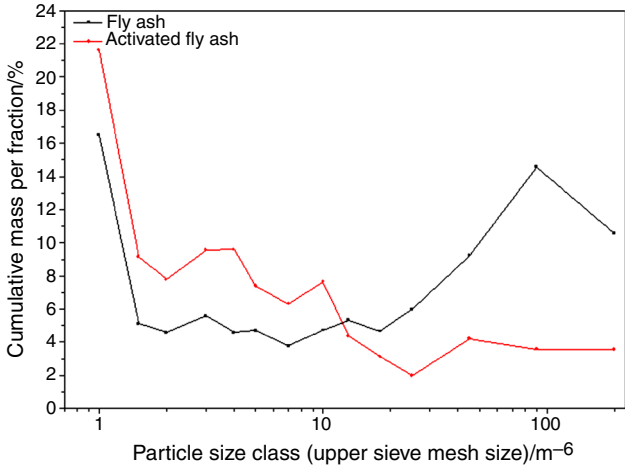

Fig. 1 The particle size grading curves of the original and activated fly ash sample

diameter of the vibrating plate is 155 m^{-3}; and engine characteristics are 380 V, 50 Hz, 750 W, and 1,000 rotations per min. The grinding material is placed into a grinding barrel, and by means of horizontal vibrations the material is ground by impact and friction, at the same time being homogenized. Grinding material used in the experiment was chrome steel 60HRC, and usable volume of grinding barrels was 100 cm^3. The activation period was selected to last 15 min based on previous researches [21–23]. Fly ash particles fraction content was analyzed by means of a multichannel coarseness analyzer Coulter Electronics Multisizer (Beckman Coulter International SA, Switzerland). Specific surface area of the ash was determined via Brunauer–Emmett–Teller (BET) method.

The C and CFA concretes were designed with different water/binder (w/b) ratios. The grain size gradings of the aggregate were selected to have matching sieve-passing ranges to eliminate the effect of grading difference on concrete properties. A goal was to obtain a strong cement matrix which fully surrounds aggregates merging them in a compact high-strength composite. The green mixes were made to obtain a slump of 150 m^{-3}. The w/b ratios were kept as low as possible retaining the optimal workability of the mixture so the more compact composite structure would be achieved. Concrete mixtures were produced according to SRPS EN 1402-5:2009 [24, 25]. The details of mixture proportions are given in Table 2.

Table 2 Mix-design of the corundum refractory concretes

Concrete	Content of particular raw material/%				Water/binder ratio
	Binder		Admixture[a]	Aggregate per fraction: 5–3; 3–2; 2–1; 1–0.5; 0.5–0 m^{-3}	
	Fly ash	Cement			
C	–	20	1	10; 20; 20; 20; 10	0.57
CFA	20	10	1	10; 20; 20; 15; 5	0.59

[a] Total concrete mass

Mixtures were homogenized using a laboratory pan-type mixer 65-L0006/AM (Controls Inc., USA). The procedure was conducted in two steps regarding water addition in order to prevent segregation. The initial sequence started with dry mixing of aggregate with binder for 2 min, after which the 80 % of water and the admixture were added and homogenized for 3 min. After the mixture rested for 2 min, remaining part of water was added and mixture was homogenized for additional 2 min. The specimens were cast in steel molds (160 × 40 × 40 m^{-3} prisms and 200 × 200 × 200 m^{-3} cubes) by a self-flow method. The molded samples were kept covered with a plastic sheet to

prevent water loss for following 24 h. After demolding, the samples were dried at 110 °C for 24 h. Dry samples were submitted to thermal treatment in a laboratory furnace at various temperatures up to 1,400 °C with 2 h delay at each temperature. Physical and mechanical properties, i.e., bulk density, porosity, crushing, and flexural strength, were tested on the prepared concrete prisms or cubes [26–29]. Total porosity was estimated by a mercury porosimeter Pascal 440 (Thermo Fisher Scientific, Inc., USA) with a pressure applied up to 200 MPa. Thermal properties (refractoriness and refractoriness under load) were tested on the samples of adequate shape and dimensions cut from the original concrete specimen [30, 31].

The differential thermal analysis was performed using the Shimadzu DTA-50 apparatus. Approximately, 30 mg of a sample was used for each DTA test along with α-Al_2O_3 powder as a reference sample. The sample was initially heated under an air atmosphere from 20 up to 1,100 °C at constant heating rate of 10 °C min^{-1}. The kinetic parameters in thermal analysis are evaluated either by single heating rate method or multiheating rate method. In this investigation, the Kissinger method based on the change in the position of the peak maxima with the heating rate was applied [32–34]. The method is well known for its easy applicability and the possibility to get a reliable value for the activation energy of several processes even if the reaction mechanism is uncertain. In thermal analysis, the expression that shows the variation of reaction rate with temperature is given as [32–34]:

$$\frac{\mathrm{d}\alpha}{\mathrm{d}t} = f(\alpha) \cdot k(T), \tag{1}$$

where α is extent of the reaction; $f(\alpha)$ is the function representing the reaction mechanism [33]; $k(T)$ is the rate constant at temperature T which has Arrhenius equation form [32]:

$$k(T) = A \exp\left(-\frac{E_\mathrm{a}}{RT}\right), \tag{2}$$

where A is the pre-exponential factor or frequency factor in min^{-1} (theoretical value is $A = 1 \times 10^{10}$ s^{-1}); E_a is the apparent activation energy of the transformation in kJ mol^{-1}; R is the gas constant (8.314 kJ mol^{-1} K^{-1}); and T is the absolute temperature in K.

The reaction rate equation (Eq. 1) and the Arrhenius equation (Eq. 2) are commonly combined into the general rate equation [32–34]:

$$\frac{\mathrm{d}\alpha}{\mathrm{d}t} = Af(\alpha) \exp\left(-\frac{E_\mathrm{a}}{RT}\right). \tag{3}$$

By performing diffraction by parts of the (Eq. 3) and further transformations as given in the literature [32–34], a final form of Kissinger equation is obtained:

$$\ln\left(\frac{\beta}{T_\mathrm{p}^2}\right) = \ln\left(\frac{AR}{E_\mathrm{a}}\right) - \frac{E_\mathrm{a}}{RT_\mathrm{p}}, \tag{4}$$

where β is a constant heating rate ($\mathrm{d}T/\mathrm{d}t$) in K min^{-1} and T_p is the maximal absolute temperature at which the reaction peak/maximum occurs, in K. Peak temperatures can be found by changing the heating rate. The activation energy and other regression parameters can be calculated from the linear regression of $\ln(\beta/T_p^2)$ versus $1/RT_p$ dependence. Namely, in the $\ln(\beta/T_p^2)$ versus $1/RT_p$ plot, the data points lie on a straight line whose slope represents E_a of the process [33, 35]. Heating rates in the experiment were chosen in accordance to the literature [32–36] and they were set as 10, 20, and 30 °C min^{-1}.

The mineralogical compositions changes were analyzed by X-ray powder diffraction method on a Philips PW-1710 automated diffractometer using a Cu tube operated at 40 kV and 30 mA. The instrument was equipped with a diffracted beam curved graphite monochromator and a Xe-filled proportional counter. The diffraction data were collected in the 2θ Bragg angle range from 5° to 70°, counting for 1 s (qualitative identification) at every 0.02° step. The divergence and receiving slits were fixed as 1 and 0.1, respectively. The microstructure was analyzed with a scanning electron microscope JEOL JSM-5800. Concrete samples were crushed, and non-polished parts covered with gold powder were used in the investigation.

Results and discussion

The mechanical activation of the fly ash took place in a vibratory disk mill as it was previously described in the Experimental Chapter. The characteristics of a product of mechanical activation are predominantly a function of the activator type and its operation kinetics. The activation is conducted in order to diminish the particle size and to obtain a higher level of homogeneity and fineness of the ash. The considered ash fineness-related parameters were mean particle diameter (d_{50}/m^{-6}), sieve mesh size appropriate to 95 % cumulative undersize of the micronized product, (d_{95}/m^{-6}), and specific surface area (SSA/m^2 kg^{-1}). The particle size-related parameters were experimentally obtained on a Coulter multisizer device, and specific surface area was obtained according to BET method. The activated ash particle size grading curve is illustrated in Fig. 1.

From the comparison of the diagrams given in Fig. 1, it can be noticed that the content of ultra-fine particle size fraction 0–1 m^{-6} increased from 16.5 to 24.99 % giving the significant rise in SSA parameter as well. Namely, the initial ash specific surface area was 267.0 m^2 kg^{-1}, and

after 15 min of activation SSA increased almost two and the half times reaching the value of 596.0 m^2 kg^{-1}. Normally, higher SSA means better reactivity of the ash. With increased reactivity and with percentage of SiO_2 in ash as high as 55.15 %, an important criterion for the pozzolanic reaction in concrete is being fulfilled. Therefore, it can be assumed that fly ash will be able to take over the binding role at ambient temperature. Regarding fly ash over-all reactivity, besides the presence of silica, the content of aluminates that could react with the lime and the soluble alkalis at ambient temperature is very important [37]. Furthermore, the high content of alumina (19.32 %) and low content of Fe oxide are also a prerequisite for achieving high refractoriness. Visual examination of the activated ash revealed that the material appeared homogenous, of even gray color, and without any noticeable agglomerations present. The fineness degree may be evaluated indirectly by measuring SSA; however, d_{50} and d_{95} parameters are the direct represents of a material fineness. The mean particle size significantly diminished starting from 82.66 to 4.35 m^{-6} after activation. The d_{95} parameter which initially amounted as high as 334 m^{-6} decreased to 12.25 m^{-6} after activation. The decrease noticed in the d_{50} and d_{95} parameters is a reliable proof of improved fineness of the activated ash.

Regarding mineralogical composition of the initial fly ash, the main crystalline phases present at ambient temperature are quartz and mullite, while calcite, magnetite, hematite, fluorite, and anhydrite are immanent in negligible amounts [23]. Fly ash also contains a certain quantity of a glassy amorphous phase [23]. Since the mechanical activation induces disorder in the material structure and generates crystal lattice defects or meta-stable forms, it can be assumed that the activation treatment brings about the reduction of the crystallinity [38]. The thermal treatment of ash promotes the increase in crystallinity of present mineral phases, and initiates formation of cristobalite as a new thermally stable mineral phase with high-melting point which eventually contributes to the thermal stability of the fly ash and ash-based composite, i.e., refractory concrete in this case [12].

The influence of mechanical activation on the processed fly ash as a componential material and on a composite in which ash is incorporated was further investigated through comparison of physical, mechanical, and thermal properties of refractory concrete specimens C and CFA prepared according to the mix-design given in Table 2. The experimentally obtained bulk density of the control sample C at ambient temperature was 2,850.0 kg m^{-3}. After exposure to 1,400 °C, the bulk density of the same sample was 2,450.0 kg m^{-3}. The bulk densities for CFA sample were slightly higher amounting to 2,920.0 and 2,460.0 kg m^{-3} at ambient and maximal temperature, respectively.

Exposure of the cementitious materials to the elevated temperatures is associated with a number of chemico-physical transformations which affect the stability of the internal structure and influence the strength of material. The causes of these transformations are dehydration and/or decomposition of the cementitious compounds, different expansion values of the constituents, i.e., thermal mismatch, and internal pore pressure. The behavior of the investigated concrete mixes C and CFA under mechanically induced load is quantitatively evaluated by measuring the compressive (CS) and flexural (FS) strengths upon heat exposure. Nine different temperatures chosen for testing were as follows: 300, 500, 800, 900, 1000, 1100, 1200, 1,300, and 1,400 °C. Before CS and FS testings were conducted, a qualitative inspection for possible defects, i.e., visible cracks and fractures or melted inclusions, on thermally treated C and CFA samples was performed. Visual observations revealed soundness of all C and CFA specimens. Namely, no spalling or disintegration was noticed due to adopted high water/binder ratios which enabled generation of more connected pores in refractory concretes and thusly caused lower internal pore pressure. Even distribution of pore pressure within connected pore channels prevented internal strains which could cause destruction of a concrete sample. The evolution of CS and FS in C and CFA samples in correlation with the temperature is illustrated in Fig. 2.

The compressive strengths achieved at ambient temperature were 58.2 and 62.0 MPa for C and CFA, respectively. The initial flexural strength for C sample was 17.2 MPa, and 18.0 MPa for CFA. The evolution of CS and FS during drying period from 20 to 110 °C in both investigated concretes showed significant decrease over the strengths at ambient temperature. This can be attributed to the evaporation of free water that leads to increase in friction between failure planes and thermal mismatch between concrete component materials [39, 40]. The initial strength abatement is followed by a somewhat slower but continuous decrease measured upon heating to temperatures up to 800 °C. At 300 °C, the CS and FS of both concrete mixes are evidently affected by the temperature, decreasing to approximately two-thirds of initial values at ambient temperature. During 500–800 °C interval, the possible chemical transformations include decomposition of the cementing compounds—calcium aluminates and alumina hydrates with its different phases, and α- to β-quartz transformation. These changes usually affect the volume occupied by cementitious products and when they are combined with the weakened cohesion between the mixture constituents induced by different expansions a net of microcracks inside the concrete mass develops. This consequently causes the degradation of the strength results [41, 42]. The lowest strength values were recorded for the

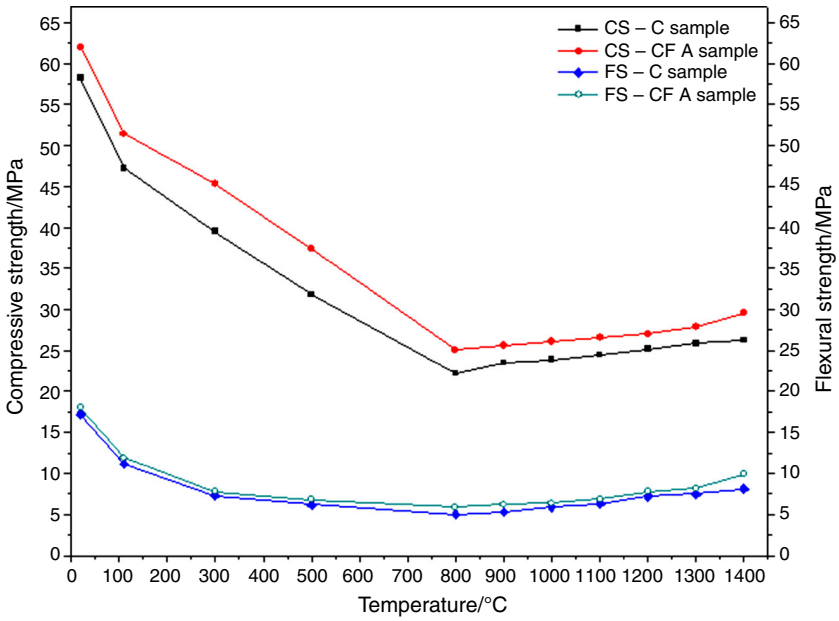

Fig. 2 Compressive and flexural strength evolution as a function of temperature

C and CFA samples thermally treatment at 800 °C, which is in consistence with previous conclusions. Namely, due to the dehydration and decomposition of cementitious products, the hydraulic bonds in concretes are being weakened, reaching the lowest point at 800 °C [41]. Exposure of a concrete to higher temperatures generally causes more chemico-physico transformations to take place, like for example recrystallization of new compounds, and additional expansions or shrinkage between the concrete constituents [43]. Namely, hydraulic bond which primarily existed between cementitious products exceeds into ceramic bond which eventually ends with sintering process. Therefore, during 800–1,400 °C interval, a slight increase in the strengths appeared. The CS values obtained at 1,400 °C were 26.3 and 29.6 MPa, for C and CFA, respectively. FS at 1,400 °C of C sample was 8.1 and 9.9 MPa for CFA. From the results given in Fig. 2, it can be seen that concretes with ash addition did not only reached mechanical characteristics of the control refractory concrete sample, but they also surpassed the given CS and FS values on all temperatures of the investigation.

The fly ash contribution to the compressive and flexural strength seems to be more efficient at higher temperatures, especially around 800 °C when significant differences between strength values for C and CFA were noticed. Apparently, during period of cementitious minerals decomposition at elevated temperatures in control concrete sample, the fly ash replacement in CFA added to the degradation resistance. Namely, addition of activated ultrafine ash promoted advancement in ceramic bounding process by providing extra componential material (especially reactive SiO_2 and Al_2O_3) for reactions. The result of these reactions is formation and/or recrystallization of mineral compounds which are able to sustain the negative influence of elevated temperature to which concrete is exposed and to preserve part of the mechanical strength. On the other side, the activation procedure also influenced increasing in SSA which in return enhanced the reactivity of ash compounds and contributed to the accelerating of the mentioned reactions in CFA.

The BET method was performed to determine the total porosity of the C and CFA concretes and to estimate the effect of the fly ash on the size of the pores in the specimens treated at different temperatures. The accumulative pore volume (P) and mean pore diameter (MPD) of the C and CFA specimens recorded at different exposure temperatures are illustrated in Fig. 3.

The initial values of the porosity were 10.8 and 9.2 % for the C and CFA specimens, respectively. After thermal treatment at 1,400 °C, the porosity ascended to 27.2 % for C, and 24.6 % for CFA sample. Estimated values for MPD at ambient temperature were 67.0 and 61.0 m^{-6} for C and CFA samples, respectively. At 1400 °C, MPD was higher than initial ones by being 86.0 m^{-6} for C and 78.0 m^{-6} for CFA. However, the highest MPD values were obtained at 800 °C: 92.0 and 87.0 m^{-6}, while P was 31.4 and 30 % for C and CFA, respectively. From the diagrams in Fig. 3, it can be concluded that the concrete with incorporated activated ash showed reduced volume of pores and smaller MPD compared to control specimen prior to high-temperature exposure as well as after exposure. Therefore, in CFA, the ash particles had role of microfiller.

Exposing CFA and C samples to temperatures up to 500 °C resulted in an obvious increase of pore volume and mean pore diameter. Due to the thermal mismatch between cement matrix and corundum aggregate, a net of

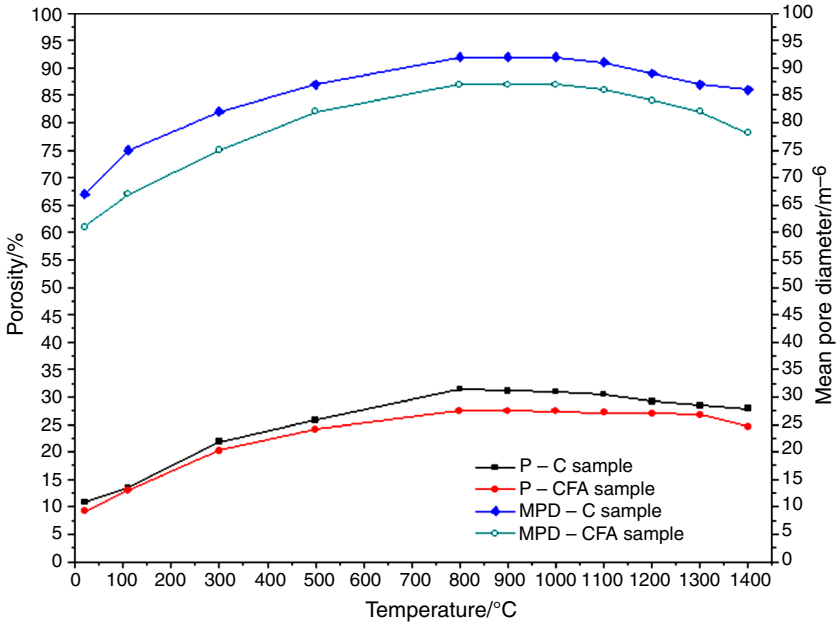

Fig. 3 Porosity and mean pore diameter evolution as a function of temperature

microcracks and microvoids is being formed which contributed to the amplification of over-all pore volume, and deepening and widening of existing pores. This effect is followed by the decrease in the CS and FS of both concrete samples as it can be seen from the comparison of Figs. 2 and 3, as well as in other researches [3, 43]. Exposing the C and CFA samples to 800 °C and temperatures above resulted in the opposite effect on the specimens total pore volume. Namely, the pores started showing a slow decrease in volume and size, but the values were still higher than those of specimens exposed to 500 °C. Specimen with incorporated activated ash had smaller total pore volume after exposure to 800 °C with respect to the control specimen, probably due to the greater stability of the hydration products against dehydration. The fly ash normally provides additional content of SiO_2 and Al_2O_3 that enables the formation of mullite in the concrete. The activation procedure additionally enhances the reactivity of the ash components and therefore increases the quantity of the reaction products. Mullite is a mineral which possesses a needle-like crystals and it usually forms a kind of crystal-net structure which fills out the thinnest pores and therefore reduces the porosity. Besides obvious influence on the reduction of the porosity, the mullite induces the increase in mechanical strengths by performing a microreinforcement role in the microstructure. Above 1,000 °C, the crystallization of calcium aluminates and subsequent consolidation of newly formed crystals are taking place in both types of concrete. The crystals are filling out voids and microcracks. This also induces the increase in mechanical strengths and contributes to materials resistance to deterioration. These high-temperature processes are initiation to sintering. The sintering takes place at the highest temperatures and improves the properties of the material by making the structure more compact. Therefore, significant shrinkage of pores, closing of the microvoids, and reduction of porosity values are expected to occur at temperatures above 1,400 °C in both investigated concretes. However, during 1,300–1,400 °C interval, a more prompt increase in strengths and the decrease in P and MPD are noticed which can be correlated to the effect of early sintering process. These effects are more pronouncedly exhibited in CFA sample, and they can be attributed to the increased ash reactivity due to the mechanical activation and the consequent influence it has on the decreasing of the sintering temperature and speeding up the sintering rate [12, 14, 44].

Both concretes showed exquisite thermal resistance. C sample showed refractoriness as high as 1,755 °C (34 SK), while CFA was thermally resistant at 1,780 °C (35 SK). Refractoriness under load of 0.2 MPa expressed as temperature of softening-initiation/end-of-softening, i.e., T_a/T_e was 1,450/1,600 °C for C and 1,480/1,630 °C for CFA. Therefore, the "recycled" concrete answered thermal stability request for the standard castables. High refractoriness of CFA was induced by additional content of alumina (19.32 %) in fly ash composition. The Fe oxide content in CFA was as low as 0.13 %, which is important because Fe_2O_3 is causative agent for production of solid solutions. The ability of the ash-based concrete to sustain exposure to elevated temperature and to match mechanical characteristics, temperature resistance, and stability of control sample is also endorsed by the presence of the additional content of mineral compounds with high-melting point—mullite and cristobalite originating from the fly ash.

Table 3 Thermally induced mineral phase changes in C and CFA concretes

Concrete	Mineral phase	Temperature/°C					
		20	300	500	900	1,100	1,400
C	Corundum (α-Al_2O_3)	+	+	+	+	+	+
	Corundum (β-Al_2O_3)	+	+	+			
	Tobermorite ($Ca_5Si_6(OH)_{18}\cdot 5H_2O$)	+	+				
	CA ($CaO\cdot Al_2O_3$)	+	+	+			
	CA2 ($CaAl_2O_4$)	+	+	+	+	+	
	CA4 ($CaAl_4O_7$)	+	+	+	+	+	
	CAH ($CaAl_2O_4\cdot 10H_2O$)	+	+				
	Quartz (SiO_2)	+	+	+	+	+	
	Gehlenite ($Ca_2Al_2SiO_7$)				+	+	+
	Anorthite ($Ca_2Al_2SiO_2O_8$)				+	+	+
CFA	Corundum (α-Al_2O_3)	+	+	+	+	+	+
	Corundum (β-Al_2O_3)	+	+	+			
	Tobermorite ($Ca_5Si_6(OH)_{18}\cdot 5H_2O$)	+	+				
	CA ($CaO\cdot Al_2O_3$)	+	+	+			
	CA2 ($CaAl_2O_4$)	+	+	+	+	+	
	CA4 ($CaAl_4O_7$)	+	+	+	+	+	
	CAH ($CaAl_2O_4\cdot 10H_2O$)	+	+				
	Quartz (SiO_2)	+	+	+	+		
	Gehlenite ($Ca_2Al_2SiO_7$)				+	+	+
	Anorthite ($Ca_2Al_2SiO_2O_8$)				+	+	+
	Cristobalite (SiO_2)					+	+
	Mullite ($Al_6Si_2O_{13}$)				+	+	+

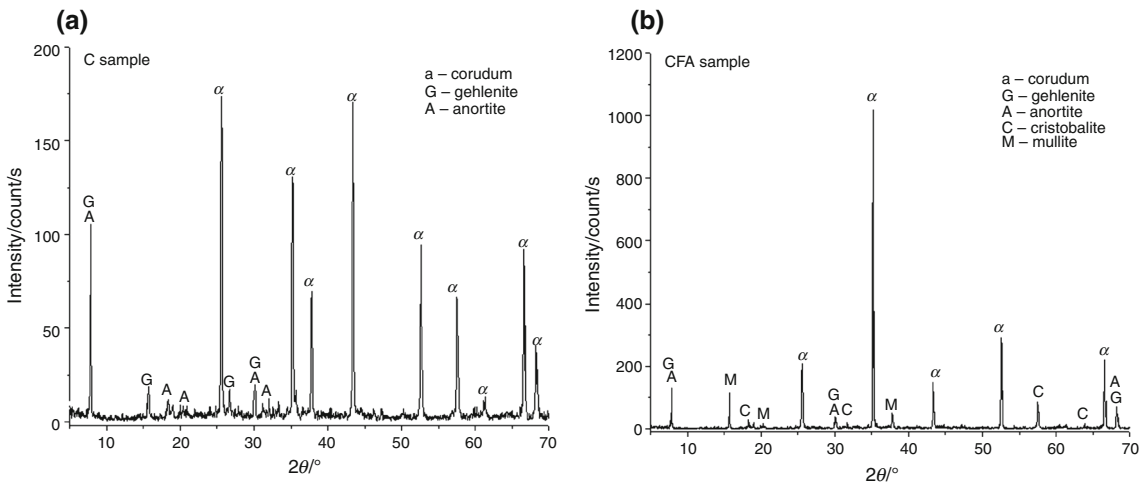

Fig. 4 XRD diffractogram of concrete samples after thermal treatment at 1,400 °C: **a** C concrete; **b** CFA concrete

The thermally induced evolution of mineral phases in C and CFA concretes is presented in Table 3. The XRD diffractograms of the C and CFA samples after thermal treatment at 1,400 °C are presented in Fig. 4.

As it can be seen in Table 3, aluminum cement minerals CA2, CA4 and CAH, and tobermorite were present in both concrete samples at lower temperatures of investigation and up to 500 °C. Above 800 °C, two new mineral phases—gehlenite and anorthite—were identified. These phases were present not only at 900, but also at 1,100 and 1,400 °C. Since gehlenite is one of the main ceramic minerals, it can be considered responsible for creation of the ceramic bond at temperatures above 800 C. By such it contributes to the increase of compressive and flexural strengths of C and CFA as is shown in Fig. 2. Gehlenite was more abundant than anorthite at the highest

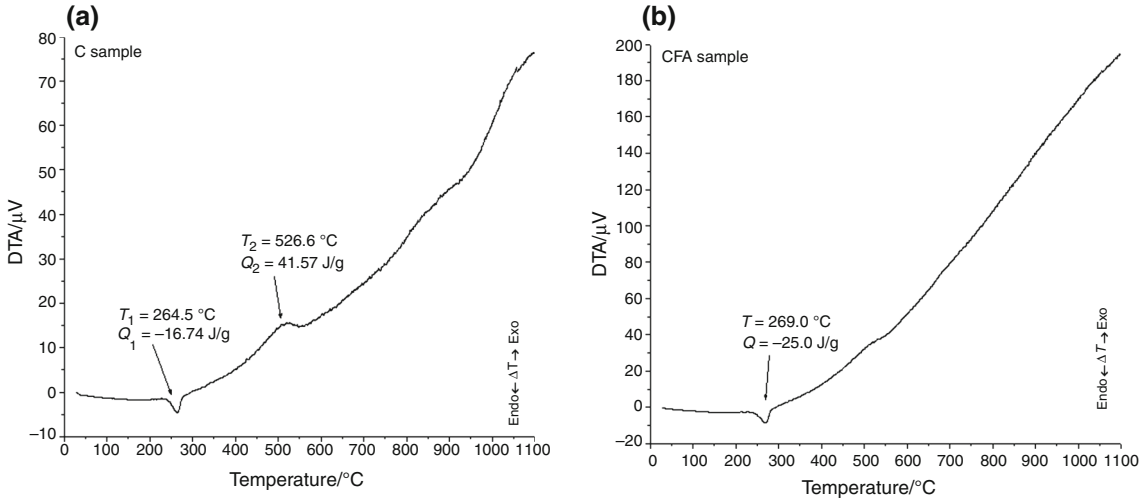

Fig. 5 DTA curve of: **a** C concrete; **b** CFA concrete

temperature of investigation in both concrete samples. In concrete with incorporated fly ash, gehlenite phase was also more abundant at 900 °C than in control sample due to the additional reactive material originating from the fly ash. Increased content of gehlenite contributed to the higher mechanical strength values of CFA concrete in comparison to C sample. The most abundant mineral in both concrete samples was α-Al_2O_3 which originates from the aggregate. At 20 °C, both α- and β-Al_2O_3 were present; however, with increasing temperature, the β-phase completely transited into α-Al_2O_3. In CFA sample, mullite and cristobalite were detected at temperatures above 900 °C. Formation of mullite and cristobalite is enabled due to additional quantity of the SiO_2 and Al_2O_3 originating from the fly ash addition. Mullite and cristobalite contributed to the high refractoriness of CFA sample and the matching over-all thermal characteristics of CFA and C, as it was already concluded. These minerals are expected to appear at the highest temperatures in C sample as well; however, their peaks were not detected due to the small quantity and peak overlapping. Crystallinity degree was higher in CFA sample in comparison to the C sample, probably due to the presence of additional componential material, i.e., reactive SiO_2 and Al_2O_3, which resulted in formation and recrystallization of new mineral compounds. The mineral phases identified by XRD method confirmed conclusions and acknowledged assumptions previously given during analysis of the physical, mechanical, and thermal properties of C and CFA concretes.

The processes which take place upon heating of the C and CFA concrete samples were investigated by means of DTA and the results are illustrated in Fig. 5.

The main thermally induced processes which occur in a refractory concrete are related to the cement hydration [12, 40, 45–47]. Due to the high-melting point of corundum applied as aggregate in both C and CFA, its minerals are practically not involved in observed hydration reactions [41]. The strength and refractoriness of the used aggregate contribute to the defining of the concrete strength and refractoriness. However, a well-performed cement hydration is the main factor in shaping of the behavior of a concrete. The hydration reactions of calcium aluminate cements are very complex. The hydration of monocalcium aluminate (CA, i.e., $CaO{\cdot}Al_2O_3$), as the main aluminum cement mineral, takes place according to the reactions given below (Eqs. 5–7):

$$CaO{\cdot}Al_2O_3 + 10H_2O \rightarrow CaO{\cdot}Al_2O_3{\cdot}10H_2O \quad (5)$$

$$CaO{\cdot}Al_2O_3{\cdot}10H_2O \rightarrow 2CaO{\cdot}Al_2O_3{\cdot}8H_2O + Al_2O_3{\cdot}H_2O \quad (6)$$

$$2CaO{\cdot}Al_2O_3{\cdot}8H_2O \rightarrow 3CaO{\cdot}Al_2O_3{\cdot}6H_2O + Al_2O_3{\cdot}H_2O. \quad (7)$$

Intermediate products of CA hydration are meta-stable. The hydrates $CaO{\cdot}Al_2O_3{\cdot}10H_2O$ and $2CaO{\cdot}Al_2O_3{\cdot}8H_2O$ subsequently decompose forming a mixture of $3CaO{\cdot}Al_2O_3{\cdot}6H_2O$, $Al(OH)_3$ gel, and water. Due to the loss of water, the result of this decomposition is an increase in porosity accompanied by a decrease in strength, as it is seen in Figs. 2 and 3 for both investigated concretes. The hydration of calcium aluminate cement is more rapid than Portland cement hydration. Also, it is followed by release of greater amount of energy [48]. Besides CA, high-aluminate cement usually contains other strength-developing phases like monocalcium dialuminate (CA2) and monocalcium tetraaluminate (CA4) in the composition, as the mineralogical analysis previously confirmed (Table 3). Calcium aluminates have high initial strength, but further

recrystallization causes decrease in the concrete strength values as it is seen in Fig. 2. Mineral phases like gehlenite and anorthite contribute little to initial strengths, but they have influence on formation of ceramic bond and later increase of strength induced by temperature and on the thermal stability of the concretes. Their influence is more distinctly pronounced in the CFA concrete due to the presence of reactive components originating from activated ash addition.

The water-binder ratio used in refractory concrete mixes is usually higher than in Portland cement concretes to prevent early deterioration of mechanical properties, thus a large amount of water is retained at elevated temperatures. The DTA analysis detected a complex endothermic effect in the interval 20–300 °C in both concrete samples, since during this interval, desorption of physically adsorbed and interlayer water molecules takes place. The main endothermic peak manifested around 300 °C marking the loss of adsorbed water and/or dehydroxylation of OH octahedral bound to Ca and Al (usually in stage 240–330 °C [49]). In C sample, the peak was recorded at 264 °C and in CFA at 269 °C. This means that addition of fly ash retarded the hydration process which can be explained by high-internal porosity of ash particles and their ability to retain certain additional quantity of water required for the reactions [23, 40]. Dehydration of the calcium aluminates and the alumina hydrates is near completion at approximately 500–600 C which is normally marked by an effect on DTA curve [46]. In C sample, the peak was recorded at 526 °C; however, in CFA sample, the expected peak was diminished. The cause can be found in overlapping and/or annulling of the effects, because during the ash thermal treatment, two processes were noticed in this region: decomposition of $CaCO_3$ at approximately 500 °C and β-quartz transformation to α-quartz at 573 °C [23, 40, 50]. By increasing temperature further, an outstretched exothermal background hump is being formed in both samples. In this temperature range, solid state reactions between calcium aluminates, alumina and lime are induced [45, 51]. This leads to increase in mechanical strength of concrete, which is supported by the results in Fig. 2. The DTA analysis did not show any sign of samples melting. The sintering of the C and CFA samples is expected to start above 1,300 °C as the increase in strengths and decrease in porosity values indicated (Figs. 2, 3). Since the refractoriness of the samples is as high as 1,755 °C for C and 1780 °C for CFA, the melting is expected to start above these temperatures.

The non-isothermal DTA recordings of C and CFA concrete samples at three different heating rates (10, 20, and 30 °C min^{-1}) were performed in order to determine the change of peak transformation temperatures (Figs. 6, 7). It can be seen that with a heating rate increase from 10 to 30 °C min^{-1} in C sample, the temperatures corresponding

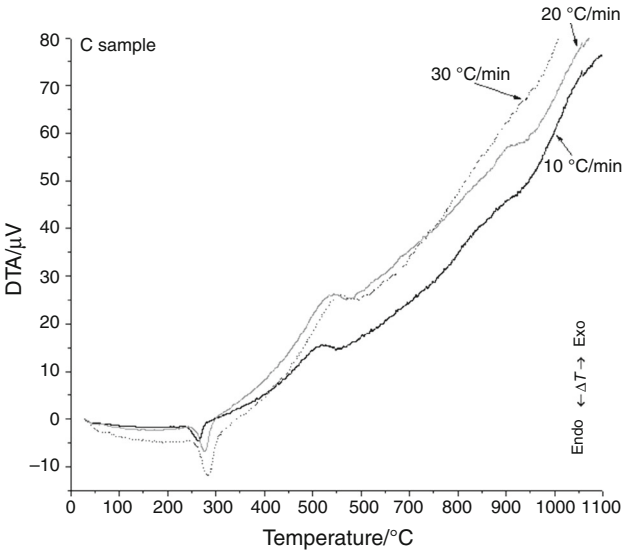

Fig. 6 DTA curves of the C concrete samples recorded at different hating rates

to the peak values increased. Furthermore, with the increase of heating rate during recording of CFA, the temperature of appropriate endothermic peak also increased. However, the second peak in the original DTA curve for CFA sample was already weak and it could not have been measured at 20 and 30 °C min^{-1} heating rates.

For the C concrete, recorded peak temperatures (T_p) at 10, 20, and 30 °C min^{-1} were $T_1^C = 264$; 280; and 290 °C, and $T_2^C = 527$; 550; and 560 °C. In case of CFA, only the first peak was distinctly visible and temperatures recorded at different heating rates were $T_1^{CFA} = 269$; 280; and 300 °C. The Kissinger's equations (Eqs. 1–4) were applied on thusly obtained T_p in order to determine the activation energies (E_a) for the processes related to peaks recorded for C and CFA samples. The plots of $\ln(\beta/T_p^2)$ versus $1/RT_p$ linear regressions are given in Fig. 8. The calculated E_a for T_1^C process was 131.554 kJ mol^{-1}, for T_2^C was 162.139 kJ mol^{-1}, and for T_1^{CFA} T_1 was 115.241 kJ mol^{-1}. The heating rate had an appreciable influence on the processes that took place in the cementitious system. As the heating rate rises, the reaction shifts to a higher temperature range, and kinetic parameters increase obviously.

By comparing T_1 processes for C and CFA samples it can be noticed that higher amount of E_a was needed for the reaction which took place in the control specimen C. Namely, the mechanical activation increased the fineness and SSA of the fly ash which in return initiated the increase of the ash reactivity, and consequently speeded up the processes which took place in ash–cement system. Also, activation energy of first T_1 step is lower than activation energy regarding second T_2 step for the same processes of

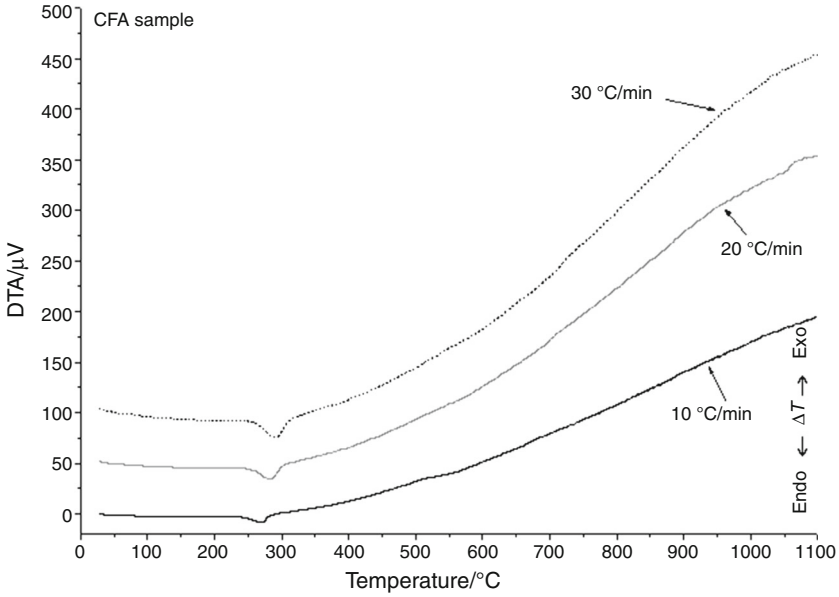

Fig. 7 DTA curves of the CFA concrete samples recorded at different hating rates

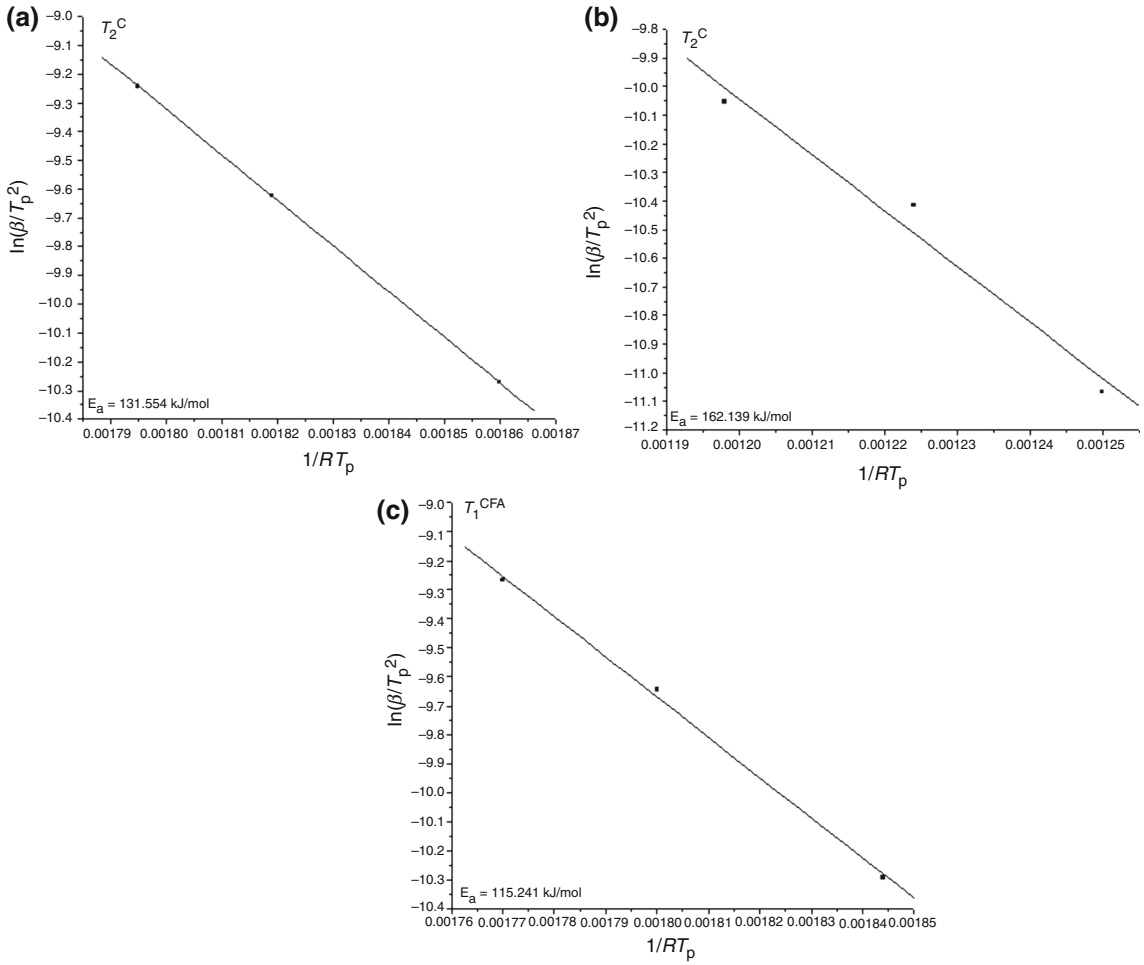

Fig. 8 Activation energy for process occurring: **a** at temperature T_1 in C sample; **b** at temperature T_2 in C sample; **c** at temperature T_1 in CFA sample

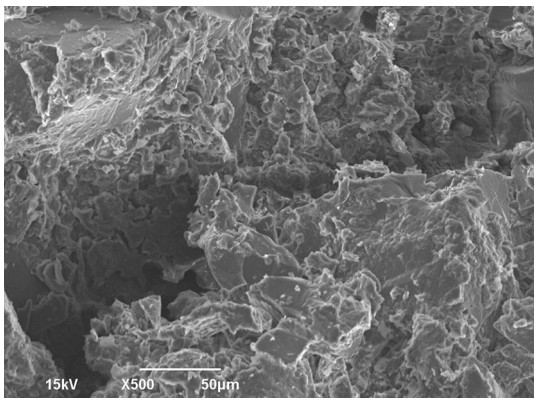

Fig. 9 SEM micrograph of concrete C after thermal treatment at 1,400 °C

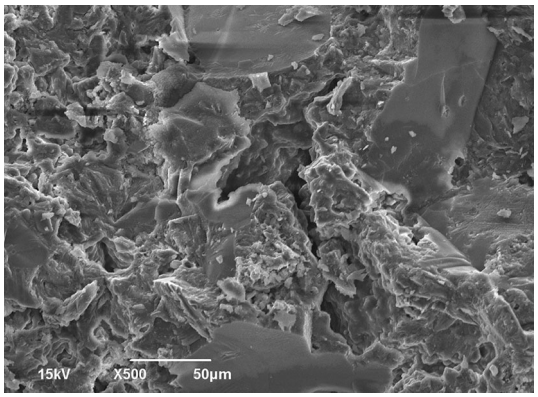

Fig. 10 SEM micrograph of concrete sample CFA after thermal treatment at 1,400 °C

dehydration in the control specimen C, owing to lower energy needed for dehydration from smaller capillary pores than from much larger gel pores, due to the decreasing of the number of water molecules present in the concrete structure during heating process. It was not possible to compare these processes in the CFA sample due to the absence of second peak as it was explained previously in DTA analysis.

The SEM micrographs of the parts of fractured C and CFA samples which were previously exposed to thermal treatment at 1,400 °C are given in Figs. 9 and 10.

The recorded microphotographs point out to the heterogeneous and multiphase microstructure characteristic for refractory concretes. Main microstructural constituents in C and CFA samples were aggregate grains, cement matrix, and thin interfacial aggregate-cement transition zone as it can be seen in Figs. 9 and 10. Fly ash particles were incorporated in CFA sample cement matrix during hardening process and therefore they cannot be distinctly visible in the SEM recording in Fig. 10. However, the effect of the activated ash addition can be observed through recorded differences in the microstructure of C and CFA samples.

In the microphotographs of both samples, corundum aggregate grains appear as huge compact surfaces surrounded by cement matrix. Aggregate grains do not contain any visible pores, voids, or microcracks due to the corundum high refractoriness and over-all stability to the temperature changes. Namely, no signs of thermally induced deterioration can be seen on the aggregate grains in any of the investigated samples. High refractoriness of the corundum contributed to over-all thermal stability of C and CFA to a large extent. The applied materials—corundum and aluminate cement in C sample, and corundum, aluminate cement and fly ash in CFA sample show no thermal mismatch, since the concrete structure after firing at 1,400 °C appears rather compact without visible delaminations and/or grouping and consequent detachments of the component grains. Furthermore, there is no visible deterioration in cement-aggregate transition zone after thermal treatment at 1,400 °C which points out to the thermal compatibility of the utilized raw materials including reapplied waste material, i.e., fly ash.

The adhesion between cement and aggregate grains in the transition zone in C and CFA concrete samples appears strong without significant porosity present. In CFA concrete, the aggregate-cement zone is composed of especially dense material (Fig. 10). Presence of air voids and other vacant spaces in this region is reduced to minimum due to the addition of fine activated fly ash particles which made the aggregate-cement connection stronger and transition zone more compact. Majority of pores in both concrete samples is located within cement matrix. From the comparison of SEM microphotographs given in Figs. 9 and 10, it can be seen that the porosity of the CFA sample cement matrix is lower and pores are smaller in comparison with control sample C which is supported by results of porosimetry testing (Fig. 3). The addition of activated ash in CFA influenced decreasing of the porosity by being partial cement replacement and enhancing the production of cementitious minerals on one side, and by being a microfiller and making structure more compact on the other side. Namely, ultra-fine ash particles practically help in "packing" of the concrete structure by filling out the voids left in inter-aggregate and cement-aggregate space. The more compact structure provides higher mechanical strengths, which was proved by mechanical testing and comparison of C and CFA concretes strengths (Fig. 2). The XRD analysis confirmed the presence of needle-like mullite crystals at high temperatures which additionally microreinforce the CFA concrete giving him higher mechanical strength. The structure of CFA is denser due to the earlier start of the sintering which induced the increase in mechanical properties as it is confirmed by

results in Figs. 2 and 3. Absence of signs of melting, i.e., glassy inclusions and liquid formations at 1,400 °C, is ascribed to the high refractoriness of the refractory concrete samples C and CFA.

Conclusions

The refractory concrete with reapplied waste raw material—fly ash (CFA) was successfully produced and its properties were compared to those of the control refractory concrete (C) with the goal to achieve matching performances. The physical, mechanical, and thermal characteristics of CFA and C concretes were studied and compared with support of DTA, XRD, and SEM results. The influence of addition of mechanically activated fly ash and firing conditions was analyzed. The major results are summarized below:

- The 15-min-long mechanical activation in vibratory mill improved the characteristics and the reactivity of the fly ash by increasing the SSA two and a half times staring from 267.0 to 596.0 $m^2 \cdot kg^{-1}$. The d_{50} as the represent of the ash fineness decreased starting from 82.66 to 4.35 m^{-6} after activation. Due to the improved characteristics, the activated ash was successfully applied as cement partial replacement and as microfiller in the CFA concrete providing it with advanced performances in comparison with control concrete C.
- The addition of activated ash improved CFA compressive and flexural strengths and reduced the porosity and the mean pore diameter in comparison to C at all temperatures from ambient to 1,400 °C. The activated ash contribution to the physical and mechanical properties was more efficient at higher temperatures when the ash replacement in CFA added to the degradation resistance by providing extra componential material (reactive SiO_2 and Al_2O_3) for formation and/or recrystallization of mineral compounds that are able to sustain negative influence of temperature and to preserve mechanical strengths.
- In CFA sample, the XRD identified extra quantity of mineral gehlenite which is by being one of the main ceramic minerals responsible for creation of strong ceramic bond, by such contributing to the increase of CFA mechanical strengths at temperatures above 800 °C. Additional quantities of mullite and cristobalite were detected in CFA due to the presence of reactive SiO_2 and Al_2O_3 from the ash. Mullite and cristobalite contributed to the high refractoriness of CFA and the matching over-all thermal characteristics of CFA and C.
- The DTA confirmed that main thermally induced processes in a refractory concretes are related to the cement hydration and detected two major two peaks: first endothermic peak at 264 °C for C and 269 °C for CFA marked the loss of adsorbed water; and second exothermic peak at 526 °C for C relates to dehydration of calcium aluminates and alumina hydrates. The first peak in CFA was shifted to higher temperature and the second peak was diminished due to the influence that ash addition has on retardation of the hydration process.
- Non-isothermal DTA performed at different heating rates and application of the Kissinger's equation in calculation of activation energies of the processes related to peak temperatures pointed out that addition of the activated fly ash influenced decreasing of the activation energy necessary for the processes.
- SEM indicated that activated ash particles improved packing of the CFA microstructure leaving a composite matrix with less structural voids in comparison to C sample. The ash showed thermal compatibility with other concrete components. Application of activated ash decreased the level of porosity and size of pores and improved mechanical strengths and over-all performances of CFA. The increase in mechanical resistance is related to the reduction in porosity, especially in microporosity, resulting in more compact structure. The sintering of the C and CFA concretes is expected to start above 1,300 °C as the increase in strengths and decrease in porosity values are indicated. Since the refractoriness of the C and CFA is above 1,750 °C the melting is not expected to start below the indicated temperature.

The recycled ash concrete CFA exhibited properties that met the requirements for the standard castables, i.e., C concrete, which proves the CFA suitable for use in severe conditions at high temperatures and highlights the reusing principle and possibility of cleaner and economically sustainable production in the industry of refractory materials.

Acknowledgements This investigation was supported by Serbian Ministry of Education, Science and Technological Development and it was conducted under projects: ON 172057 and III 45008.

References

1. Ouedraogo E, Roosefid M, Prompt N, Deteuf C. Refractory concretes uniaxial compression behavior under high temperature testing conditions. J Eur Ceram Soc. 2011;31:2763–74.
2. Simonin F, Olagnon C, Maximilien S, Fantozzi G. Room temperature quasi-brittle behaviour of an aluminous refractory concrete after firing. J Eur Ceram Soc. 2002;22:165–72.
3. Vodak F, Trtık K, Kapickov O, Hoskov S, Demo P. The effect of temperature on strength–porosity relationship for concrete. Constr Build Mater. 2004;18:529–34.
4. Tomba Martinez A, Luz A, Braulio M, Pandolfelli V. Creep behavior modeling of silica fume containing Al_2O_3–MgO refractory castables. Ceram Inter. 2012;38:327–32.

5. Chancey R, Stutzman P, Juenger M, Fowler D. Comprehensive phase characterization of crystalline and amorphous phases of a Class F fly ash. Cem Concrete Res. 2010;40:146–56.
6. Erol M, Kucukbayrak S, Ersoy-Mericboyu A. Characterization of sintered coal fly ashes. Fuel 2008;87:1334–1340.
7. Erol M, Kucukbayrak S, Ersoy-Mericboyu A. Comparison of the properties of glass, glass–ceramic and ceramic materials produced from coal fly ash. J Hazard Mater. 2008;153:418–25.
8. Biernacki J, Vazrala A, Leimer H. Sintering of a class F fly ash. Fuel. 2008;87:782–92.
9. Ilic M, Cheeseman C, Sollars S. Mineralogy and microstructure of sintered lignite coal fly ash. Fuel. 2003;82:331–6.
10. Furlani E, Bruckner S, Minichelli D, Mashio S. Synthesis and characterization of ceramics from coal fly ash and incinerated paper mill sludge. Ceram Inter. 2008;34:2137–42.
11. Acar I, Atalay M. Characterization of sintered class F fly ashes. Fuel. 2013;106:195–203.
12. Terzić A, Pavlović Lj, Obradović N, Pavlović V, Stojanović J, Miličić Lj, Radojević Z, Ristić M. Synthesis and sintering of high-temperature composites based on mechanically activated fly ash. Sci Sint 2012;44:135–146.
13. Kumar R, Kumar S, Mehrotra S. Towards sustainable solutions for fly ash through mechanical activation. Conserv Recycl. 2007;52:157–79.
14. Temuujin J, Williams R, van Riessen A. Effect of mechanical activation of fly ash on the properties of geopolymer cured at ambient temperature. J Mater Process Techn. 2009;209:5276–80.
15. Senneca O, Salatino P, Chirone R, Cortese L, Solimene R. Mechanochemical activation of high-carbon fly ash for enhanced carbon reburning. Proc Combust Inst. 2011;33:2743–53.
16. Kumar S, Kumar R. Mechanical activation of fly ash: effect on reaction, structure and properties of resulting geopolymer. Ceram Inter. 2011;37:533–41.
17. Obradović N, Terzić A, Pavlović Lj, Filipović S, Pavlović V. Dehydration investigations of a refractory concrete using DTA method. J Therm Anal Calorim. 2012;110:37–41.
18. Inoue T, Okaya K. Grinding mechanism of centrifugal mills—a simulation study based on the discrete element method. Int J Miner Process. 1996;44–45:425–35.
19. Kheifets A, Lin I. Energy transformations in a planetary grinding mill Part l. General treatment and model design. Int J Miner Process. 1996;47:1–19.
20. Shinohara K, Golman B, Uchiyama T, Otani M. Fine-grinding characteristics of hard materials by attrition mill. Powder Technol. 1999;103:292–6.
21. Terzić A, Andrić Lj, Mitić V. Assessment of intensive grinding effects on alumina as refractory compound: acceleration of γ to α phase transformation mechanism. Ceram Inter. 2014;40:14851–63.
22. Andrić Lj. Mica—preparation and application, Monograph. Publ: institute for technology of nuclear and other raw mineral materials, Belgrade 2006 (in Serbian). ISBN: 86-82867-19-2.
23. Terzić A, Pavlović Lj, Miličić Lj. Evaluation of lignite fly ash for utilization as component in construction materials. Int J Coal Prepar Utiliz. 2013;33:159–80.
24. ASTM C862-02: standard practice for preparing refractory concrete specimens by casting. 2008.
25. SRPS EN 1402-5: Unshaped refractory products, Part 5: Preparation and treatment of test pieces. 2009.
26. SRPS EN 993-1: Methods of test for refractory products, Part 1: Determination of bulk density, apparent porosity and true porosity. 2009.
27. SRPS EN 993-2: Methods of test for refractory products, Part 2: Determination of true density. 2009.
28. SRPS EN 993-5: Methods of test for refractory products, Part 5: Determination of crushing strength. 2009.
29. SRPS EN 993-6: Methods of test for refractory products, Part 6: Determination of modulus of rupture. 2009.
30. SRPS B.D8.301: Refractories—determination of pyrometric cone equivalent (refractoriness). 1974.
31. SRPS EN ISO 1893: Refractory products; Determination of refractoriness under load; differential method with rising temperature. 2010.
32. Blaine R, Kissinger H. Homer Kissinger and the Kissinger equation. Thermochim Acta. 2012;540:1–6.
33. Chen D, Gao X, Dollimore D. A generalized form of the Kissinger equation. Thermochim Acta. 1993;215:109–17.
34. Kissinger HE. Reaction kinetics in differential thermal analysis. Anal Chem. 1957;29(11):1702–6.
35. Agresti F. An extended Kissinger equation for near equilibrium solid–gas heterogeneous transformations. Thermochim Acta. 2013;566:214–7.
36. Liu F, Liu XN, Wang Q. Examination of Kissinger's equation for solid-state transformation. J Alloy Compd. 2009;473:152–6.
37. Gjorv O. High strength concrete. In: Malhotra VM, editor. Advances in concrete technology. Canada: American Concrete Institute Montreal; 1992. p. 21–77.
38. Balaz P. Mechanical activation in hydrometallurgy. Int J Miner Process. 2003;72:341–54.
39. Chindaprasirt P, Rukzon S. Strength, porosity and corrosion resistance of ternary blend portland cement, rice husk ash and fly ash mortar. Constr Build Mater. 2008;22:1601–6.
40. Terzić A, Pavlović Lj, Radojević Z, Pavlović V, Mitić V. Novel utilization of fly ash for high-temperature mortars: phase composition, microstructure and performances correlation. Int J Appl Ceram Technol 2013. doi:10.1111/ijac.12135.
41. Terzić A, Pavlović Lj. Correlation among sintering process, porosity, and creep deformation of refractory concrete. J Mater Sci 2009;44:2844–2850.
42. Tangpagasit J, Cheerarot R, Jaturapitakkul C, Kiattikomol K. Packing effect and pozzolanic reaction of fly ash in mortar. Cem Concr Res. 2005;35:1145–51.
43. Bazant Z, Kaplan M. Concrete at high temperatures. Essex: Longman; 1996.
44. Blanco F, Garcia M, Ayala J, Mayoral G, Garcia M. The effect of mechanically and chemically activated fly ashes on mortar properties. Fuel. 2006;85:2018–26.
45. Oliveira I, Ortega F, Pandolfelli V. Hydration of CAC cement in a castable refractory matrix containing processing additives. Ceram Inter. 2009;35:1545–52.
46. Pacewska B, Nowacka M, Wilinska I, Kubissa W, Antonovich V. Studies on the influence of spent FCC catalyst on hydration of calcium aluminate cements at ambient temperature. J Therm Anal Calorim. 2011;105:129–40.
47. Tongsheng Z, Qijun Y, Jiangxiong W, Peng G, Pingping Z. Study on optimization of hydration process of blended cement. J Therm Anal Calorim. 2012;107:489–98.
48. Slanicka S, Madej J, Jakubekova D. DTA contribution to study of hydration fly ash—portland cement pastes. Thermochim Acta. 1985;93(15):601–4.
49. Ukrainczyk N, Matusinovic T, Kurajica S, Zimmermann B, Sipusic J. Dehydration of a layered double hydroxide—C2AH8. Thermochim Acta. 2007;464:7–15.
50. Guo R, Venugopalan D, Rohatgi P. Differential thermal analysis to establish the stability of aluminum-fly ash composites during synthesis and reheating. Mater Sci Eng A. 1998;241:184–90.
51. Altun İ. Effect of temperature on the mechanical properties of self-flowing low cement refractory concrete. Cem Concr Res. 2001;31(8):1233–7.